SUPPLEMENTAL DATA

SUPPLEMENTAL EXPERIMANTAL PROCEDURES

Peripheral blood analysis- Eighteen-week-old mice were anesthetized with isoflurane (Baxter Healthcare, Deerfield IL). Blood was drawn from the orbital sinus using a capillary tube and then stored in an EDTA-coated tube. Blood was analyzed using a Complete Blood Count System (Drew Scientific, Dallas, TX).

Cell cycle analysis- MEFs were fixed by overnight exposure to 75% ethanol at -20°C and then stained with propidium iodide for 15 min at 4°C. Cell cycle distribution was analyzed by flow cytometry (BD Bioscience, San Jose, CA)

Semi-quantitative RT-PCR- RNA from mouse tails was extracted using Trizol (Invitrogen). Reverse transcription was performed using SuperscriptII and random primers (Invitrogen). The following primers were used for amplifying *Appl1* cDNA. For N' cDNA PCR: forward- CAT TGA AGA GAC CCT GGA GG, reverse- ACT GGG AAA TGG GGA ACA TC (within exon5). For C' cDNA PCR: forward- AGA TCT TAG CTG CTC GGG C, reverse- TGG TTT GGT CTA CTG GAG GC. The following conditions were used for PCR: denaturation at 94° C for 3 min, followed by denaturation at 94° C for 20 sec, annealing at 57° C for 30 sec, extension at 72° C for 50 sec for 30 cycles.

Real-time PCR- The quality of the RNA was measured on a BioAnalyzer. RNA was quantified using a Nanodrop UV spectrophotometer. RNA was reverse-transcribed (RT) using the M-MLV reverse transcriptase (Ambion, Austin, TX) and a mixture of anchored oligodT and random decamers. For each sample, two RT reactions were performed with 100 ng or 25 ng of total RNA in 25 µl. Aliquots (5 µl) of cDNAs were used for PCR. Real-time Taqman PCR Assays-on-Demand, from Applied Biosystems (Mm01156980_m1 for *Met* and Mm00507500_m1 for *Appl2*), were run using Universal PCR master mix from Applied Biosystems on a 7900 HT instrument. Cycling conditions were 95° C, 15 min followed by 40 cycles (95° C, 15 sec; 60° C, 60 sec) in two steps. A four points, 4-fold dilutions standard curve established with a calibrator sample was used to convert the Ct values into quantities. For each sample, the values are the means and standard deviations of data from two PCR reactions performed with the cDNAs from the two RT reactions.

SUPPLEMENTAL FIGURE LEGENDS

Suppl. Fig. 1. Tissue distribution and modification of Appl1 protein in adult mice. (A) Western blot showing Appl1 expression in various mouse tissues. Note that Appl1 bands observed with the N-terminal-specific antibody show a different pattern than with the C-terminal-specific antibody. Appl2, recognized by an N-terminal antibody, has an expression pattern similar to that of Appl1. (B) Immunoblotting for Akt1, Akt2, Akt3 and Gsk3β proteins. Note that Akt1/2 have a broad expression pattern similar to that detected with antibodies recognizing the C-terminus of Appl1. Immunoblotting for three different housekeeping proteins (QM, Gapdh, and β-actin) overall show equal loading of total protein, although tissue variations are apparent even with these loading controls.

Suppl. Fig. 2. Exon5 deletion of the *Appl1* gene abolishes Appl1 protein expression. (A) Semi-quantitative RT-PCR demonstrating that exon5 is lost in the mRNA from homozygous *Appl1-/-* mouse tails as determined using primer pairs from exon1 and exon5. However, the mutant mRNA lacking exon 5 and with an altered reading frame was expressed as shown using primer pairs specific for the C-terminus of the *Appl1* mRNA. (B) Appl1 protein is lost in various mouse tissues from homozygous *Appl1* exon5 knockout mice. In addition to Appl1, other proteins involved in the Akt pathway were analyzed by western blotting. (C) Like the homozygous exon5 knockout mice, tissues from a homozygous exon1 disrupted mouse (Tan et al., manuscript in preparation) do not express any form of

Appl1 protein, as shown by immunoblotting using antibodies against N-terminal, C-terminal, or mid-portion of Appl1.

Suppl. Fig. 3. Appl1 loss does not affect Akt stability and activation. (A) Fetal brain, lung, heart and liver from another litter at E18.5 were homogenized and submitted to immunoblot analysis of Akt1/p-Akt and Gsk3β/p-Gsk3β. (B, C) Signal densities were quantified and normalized against total Akt1 or Gsk3β, respectively.

Suppl. Fig. 4. APPL1 and APPL2 exhibit similar interaction patterns with AKT1, AKT2, AKT3, GSK3β, TSC2 and RAB5 in 293T, A2780 and IGR-OV1 cells. APPL1 and APPL2 were immunoprecipitated from these cell lysates, and immunoblot analysis was performed to detect expression of the various proteins shown.

Suppl. Fig. 5. Appl1 loss attenuates Akt activation in a growth factor-specific manner. (A) Wild-type and the *Appl1*-null MEFs were starved in media containing 0.05% FBS for 16 hr and then incubated in fresh media containing 10% FBS for the indicated times. Western blot analysis was performed to detect p-Akt, Akt1, Akt2, p-Gsk3β, Gsk3β and Gapdh. (B, C) Wild-type and *Appl1*-null MEFs were starved in media containing 0.05% fetal bovine serum (FBS) (B) or without FBS (C) for the indicated times, and western blot analysis was performed to detect p-Akt/Akt as well as p-Erk/Erk. (D) MEFs were cultured in medium containing 10% FBS, no FBS, and serum free medium with either LY294002 (15 μM), RAD001 (20 pM), PD98059 (40 μM) or RAD001 plus PD98059 for 7 h. An MTS assay was performed to assess cell viability. Stv.: serum starved; LY: LY294002; Rad: RAD001; PD: PD98059. (E-F) Activation of the Akt pathway was evaluated by analyzing phospho-Akt, phospho-Gsk3β and phospho-p70S6k levels. Activation of apoptotic pathways was investigated using antibodies recognizing cleavage of caspases 9, 3, 6, or 7 and Parp (f: full length; c: cleaved form). (G) Wild-type and *Appl1*-null MEFs were starved with DMEM containing 0.05% FBS for 30 min and then treated with 20 ng/ml EGF, for the indicated times. Expression of activated and total Akt and other components of the Akt pathway was determined by immunoblotting.

Suppl. Fig. 6. Effect of serially diluted EGF in MEFs. Serum-starved MEFs were treated with EGF (10 pg/ml, 100 pg/ml 1 ng/ml, and 10 ng/ml), and Akt activation was evaluated by immunoblotting.

Suppl. Fig. 7. Appl2 knockdown does not affect cell cycle progression in *Appl1-/-* MEFs. (A) Stealth *Appl2* siRNAs were transfected into NIH 3T3 cells stably expressing a TAP-tagged mouse *Appl2* cDNA by Nucleofection. Knockdown effect 72 hr after transfection was assessed by western blot and the knockdown efficiency was quantified as described in the "Experimental Procedures". (B) Real-time PCR analysis of *Appl2* knockdown in NIH 3T3 and *Appl1*-/- MEFs. Housekeeping Gene TATA-Binding Protein (Tbp) was used as an internal control. (C) Real-time PCR was performed to determine the knockdown effect on the endogenous *Appl2* mRNA in *Appl1*-null MEFs 72 hr post-transfection. (D) Cell cycle distribution was evaluated in wild-type, *Appl1*-null and *Appl1*-null*/Appl2* knockdown cells. (E-F) Analysis of HGF-induced Akt activation in wild-type MEFs following *Appl2* knockdown for 72 h.

Suppl. Fig. 8. Appl1/2 are required for HGF-induced transwell mobility of MEFs. Boyden chamber with PET membrane was employed to study cell migration using 10 ng/ml HGF as the chemo-attractant. Wild-type, *Appl1*-null and *Appl1*-null*/Appl2* knockdown and *Appl1*-null*/HA-APPL1* cells were used for the assay. Cells treated with HGF plus LY294002 (5 μM) were used as a negative control, and cells treated with EGF (10 ng/ml) were used as a positive control.

Suppl. Fig. 9. Appl1 is essential for HGF-induced cell survival, but does not appear to participate in general apoptotic pathways. (A) Quantified signal densities of cleaved forms of caspases 3, 6, and 7,

cleaved Parp, as well as phosphorylated Akt, Gsk3β and p70S6k of bands shown in Fig. 10B. (B) Wild-type and Appl-/- MEFs were subjected to 160 J/m^2, 10 pg/ml TNFα + 100 ng/ml cycloheximide (CHX), or 3 ug/ml Tunicamycin (TN) for 24 h, and cell viability was analyzed by MTS assay. (C) UV-induced p53 activation as well as caspase 3 and Parp cleavage were determined by western blot analysis.

SUPPLEMENTAL TABLE

Suppl. Table.1. Peripheral blood analysis of *Appl*-null mice and wild-type littermates

Hematological parameters	female mean ± SD (no. samples)		male mean ± SD (no. samples)	
	Wild-type (8)	*Appl1*-/- (4)	Wild-type (4)	*Appl1*-/- (5)
WBC(10^3/uL)	8.28 ± 3.03	8.47 ± 1.55	11.73 ± 1.23	13.22 ± 1.35
Neutrophils (%)	25.57 ± 8.99	26.28 ± 9.77	22.25 ± 4.71	23.25 ± 7.88
Lymphocytes (%)	57.81 ± 9.34	57.13 ± 12.02	64.58 ± 5.03	62.58 ± 11.18
Monocytes (%)	16.22 ± 4.01	16.14 ± 3.96	12.08 ± 2.29	13.36 ± 4.09
Eosinophils (%)	0.35 ± 0.36	0.34 ± 0.17	0.97 ± 0.64	0.76 ± 0.52
Basophils (%)	0.05 ± 0.03	0.11 ± 0.09	0.12 ± 0.17	0.05 ± 0.04
Erythrocytes (10^6/uL)	9.084 ± 0.44	9.02 ± 1.06	9.25 ± 0.72	8.79 ± 0.52
Hemoglobin (g/dl)	12.29 ± 0.68	12.38 ± 1.37	12.9 ± 0.43	11.82 ± 0.58
Hematocrit (%)	47.04 ± 6.85	47.5 ± 13.19	47.63 ± 10.38	41.7 ± 2.83
Platelets (10^3/uL)	718.6 ± 174.1	796.0 ± 243.7	835.5 ± 165.7	1036.0 ± 44.4
Mean corpuscular volume (fL)	51.86 ± 8.09	52.03 ± 7.8	51.23 ± 8.16	47.52 ± 3.52
Mean corpuscular hemoglobin (pg)	13.55 ± 0.7	13.7 ± 0.24	14.0 ± 0.88	13.46 ± 0.51
Mean corpuscular hemoglobin concentration (g/dL)	26.56 ± 3.61	26.83 ± 3.71	27.85 ± 4.62	28.42 ± 1.34

SUPPLMENTAL FIGURES

SUPPLMENTAL FIGURE 1.

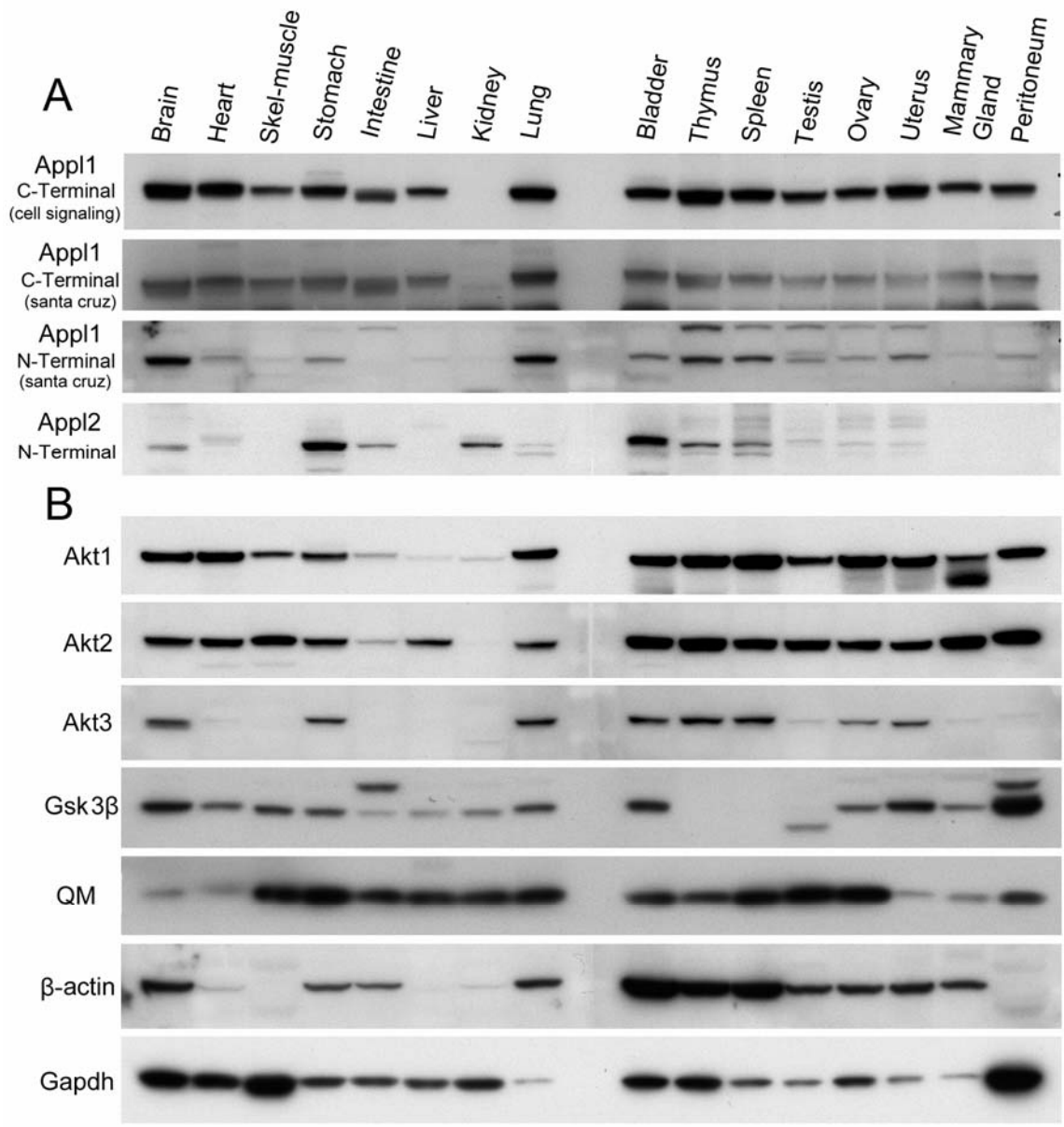

SUPPLMENTAL FIGURE 2.

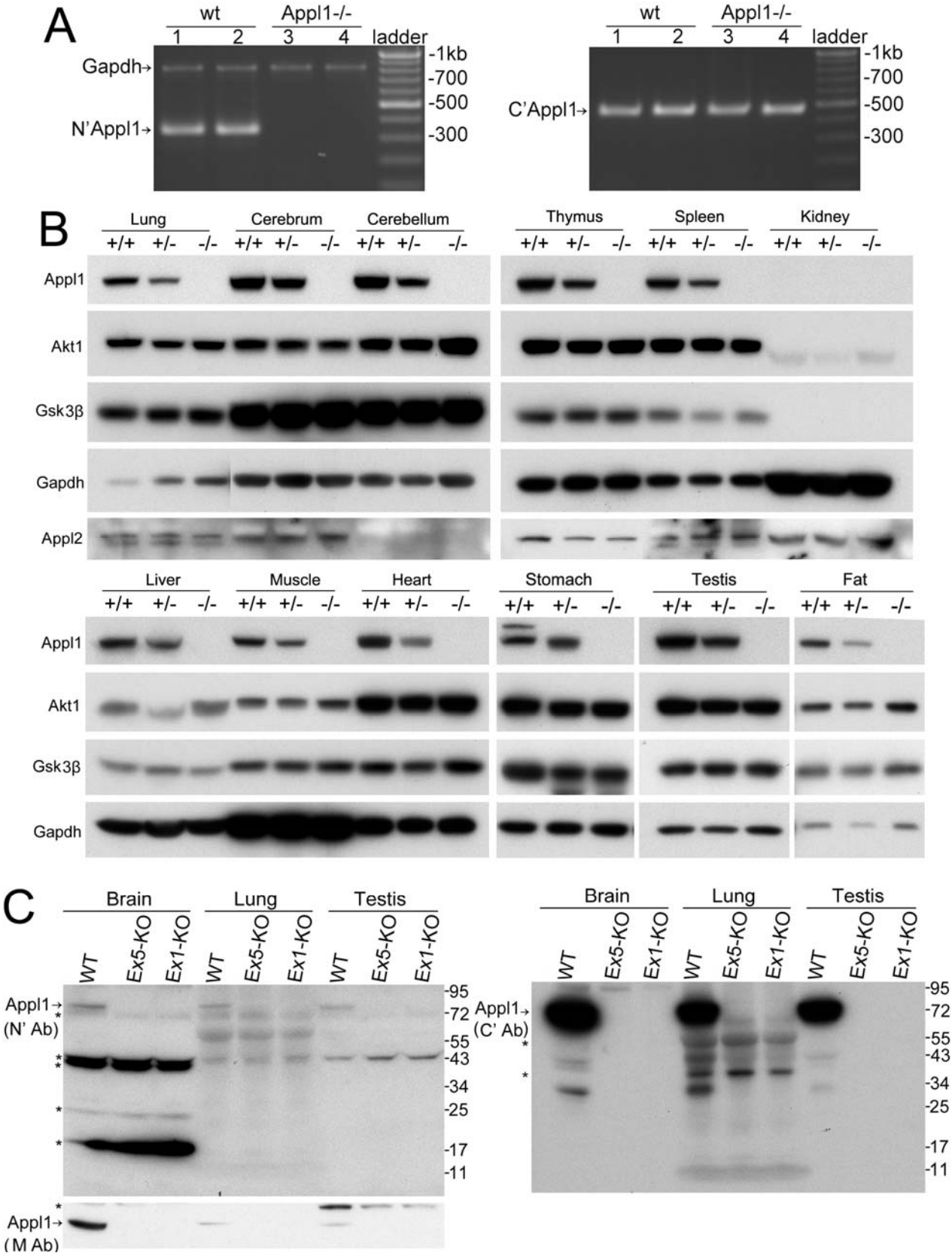

SUPPLMENTAL FIGURE 3.

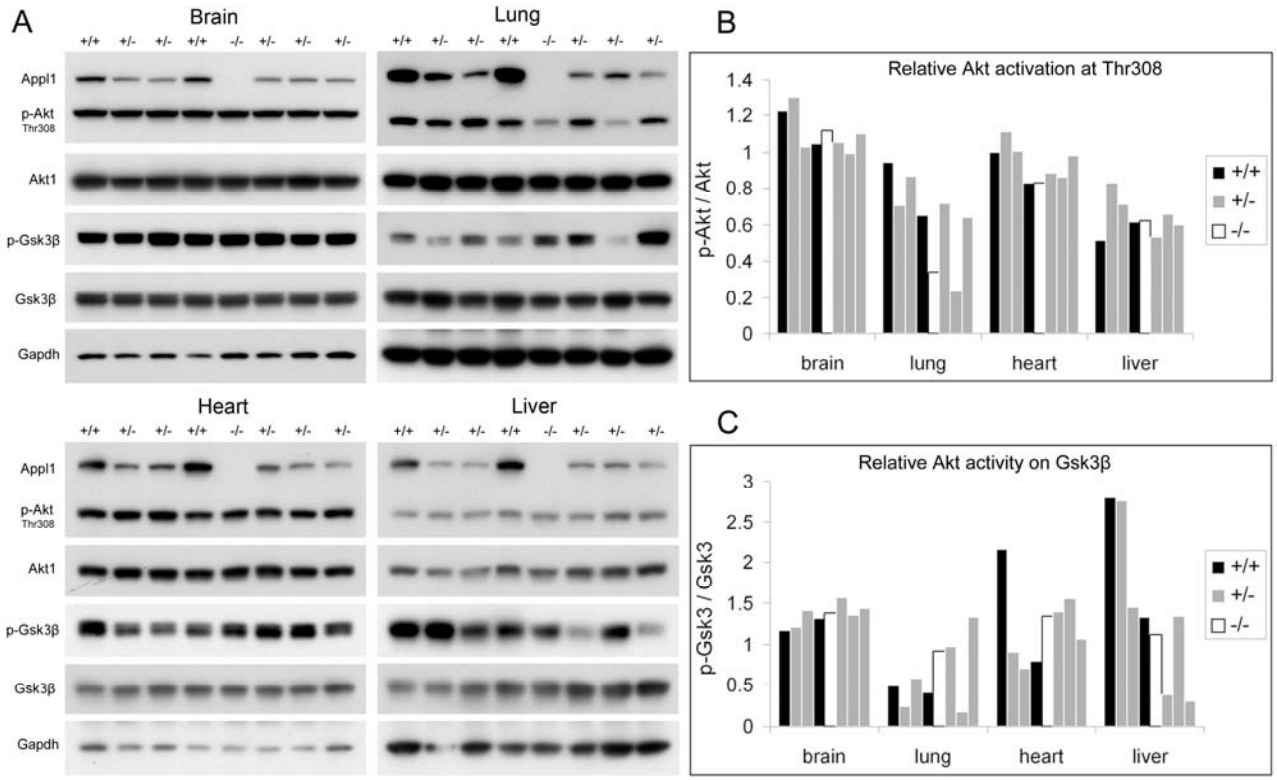

SUPPLMENTAL FIGURE 4.

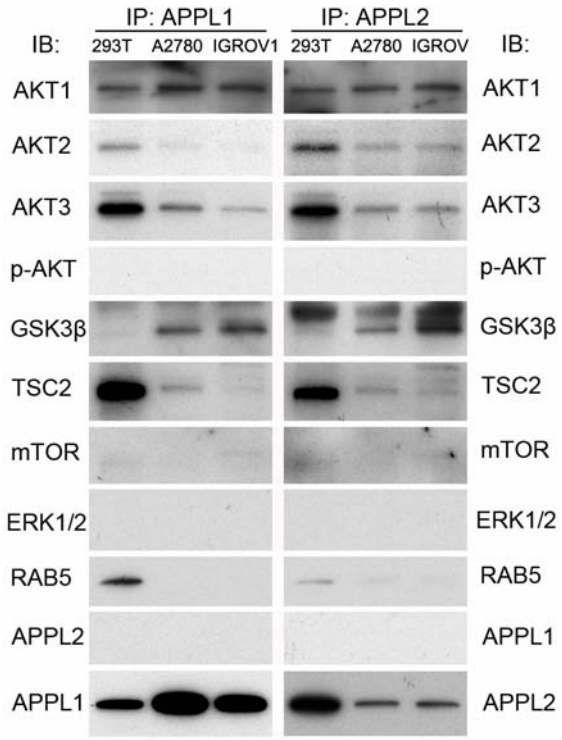

SUPPLMENTAL FIGURE 5.

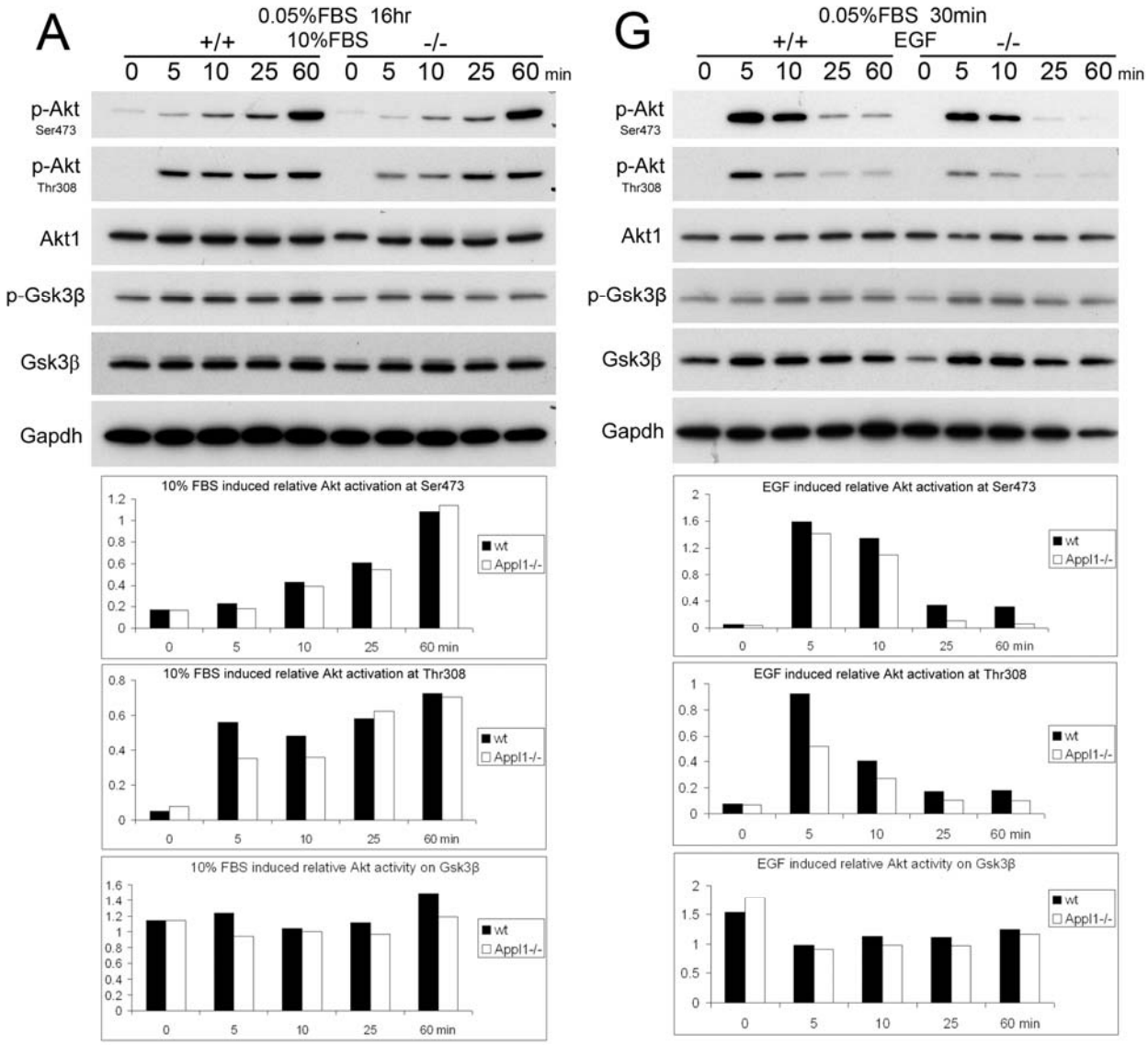

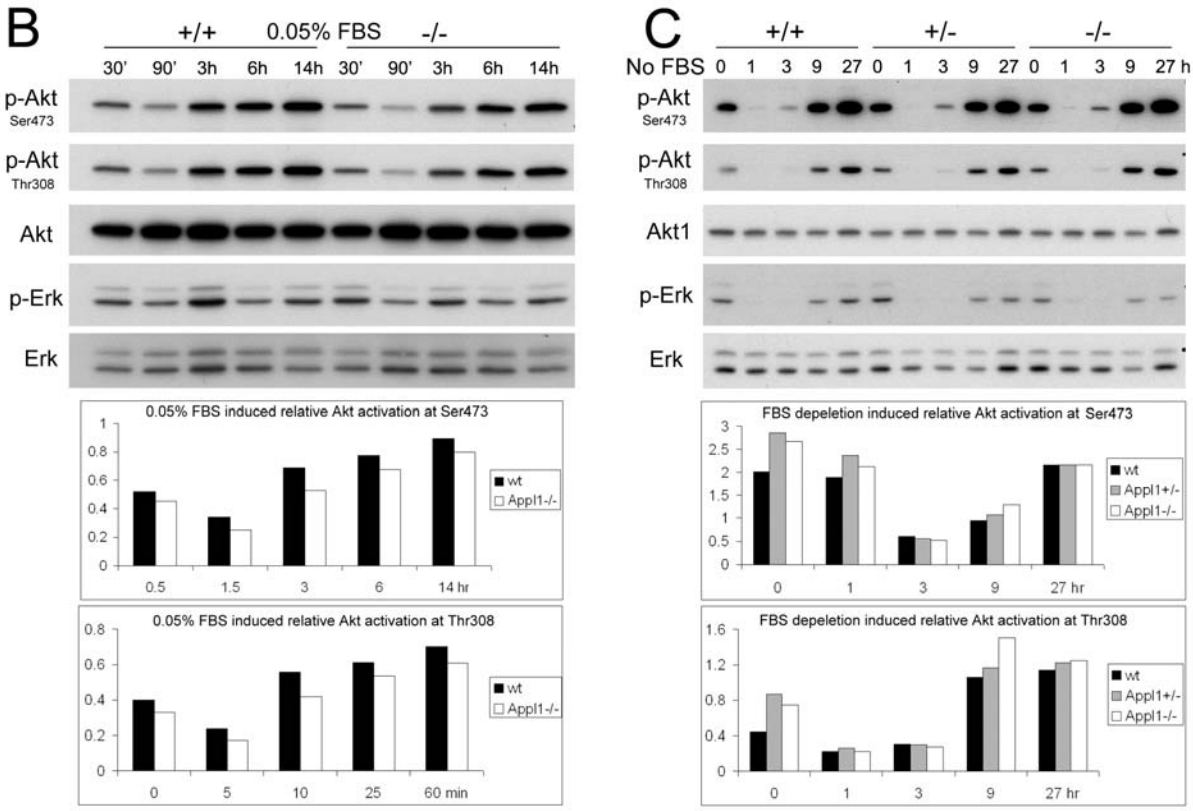
B
+/+
0.05% FBS
-/-
30' 90' 3h 6h 14h 30' 90' 3h 6h 14h
p-Akt Ser473
p-Akt Thr308
Akt
p-Erk
Erk
0.05% FBS induced relative Akt activation at Ser473
wt
Appl1-/-
0.5 1.5 3 6 14 hr
0.05% FBS induced relative Akt activation at Thr308
0 5 10 25 60 min
C
+/+
+/-
-/-
No FBS 0 1 3 9 27 0 1 3 9 27 0 1 3 9 27 h
p-Akt Ser473
p-Akt Thr308
Akt1
p-Erk
Erk
FBS depeletion induced relative Akt activation at Ser473
wt
Appl1+/-
Appl1-/-
0 1 3 9 27 hr
FBS depeletion induced relative Akt activation at Thr308
0 1 3 9 27 hr

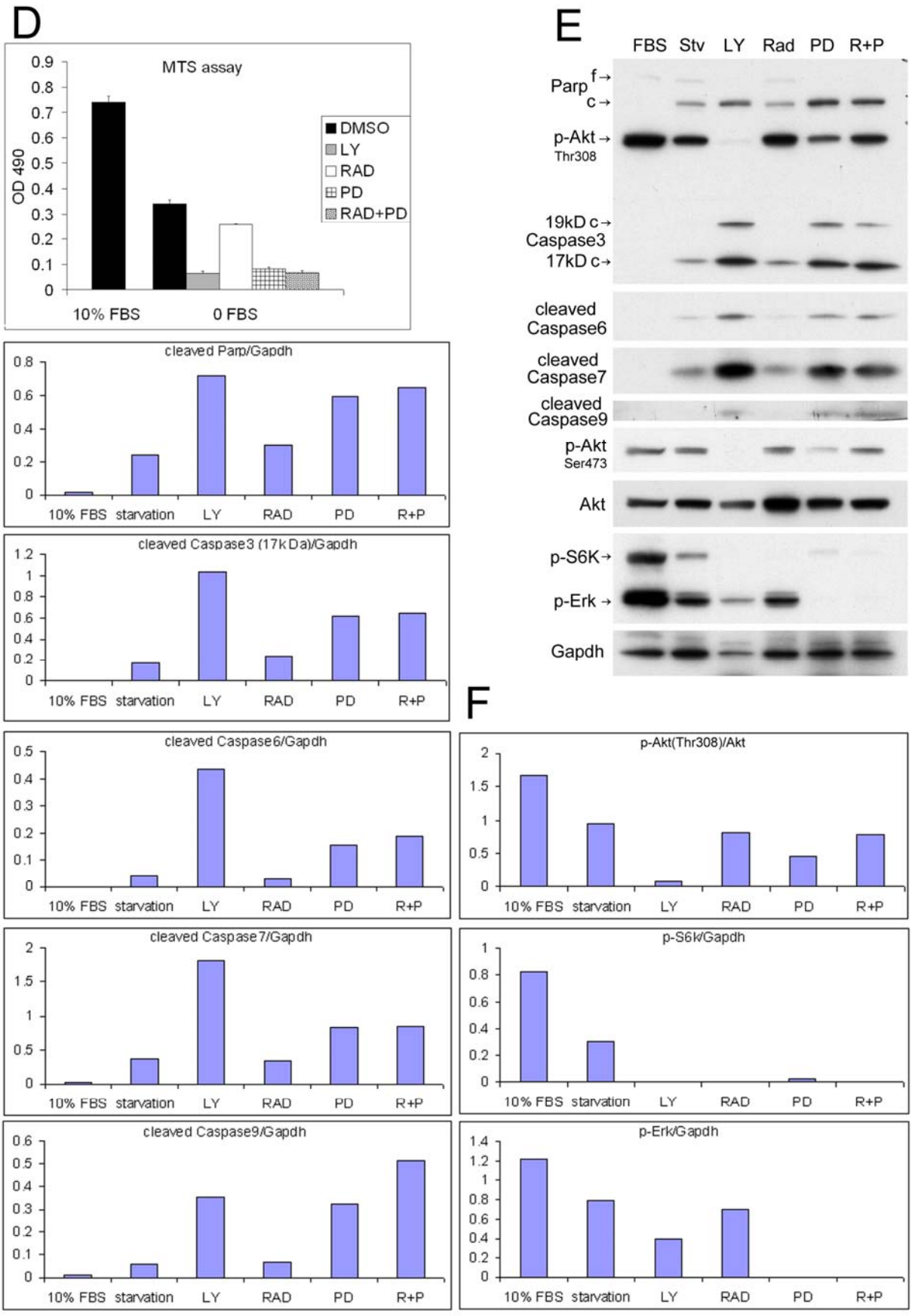
D
MTS assay
OD 490
DMSO
LY
RAD
PD
RAD+PD
10% FBS
0 FBS
cleaved Parp/Gapdh
cleaved Caspase3 (17kDa)/Gapdh
cleaved Caspase6/Gapdh
cleaved Caspase7/Gapdh
cleaved Caspase9/Gapdh
10% FBS
starvation
LY
RAD
PD
R+P
E
FBS
Stv
LY
Rad
PD
R+P
Parp f→
c→
p-Akt→
Thr308
19kD c→
Caspase3
17kD c→
cleaved
Caspase6
cleaved
Caspase7
cleaved
Caspase9
p-Akt
Ser473
Akt
p-S6K→
p-Erk→
Gapdh
F
p-Akt(Thr308)/Akt
p-S6k/Gapdh
p-Erk/Gapdh

SUPPLMENTAL FIGURE 6.

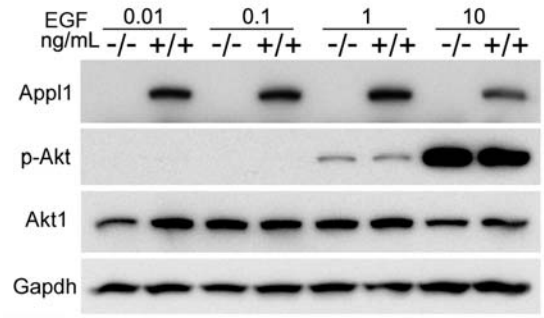

SUPPLMENTAL FIGURE 7.

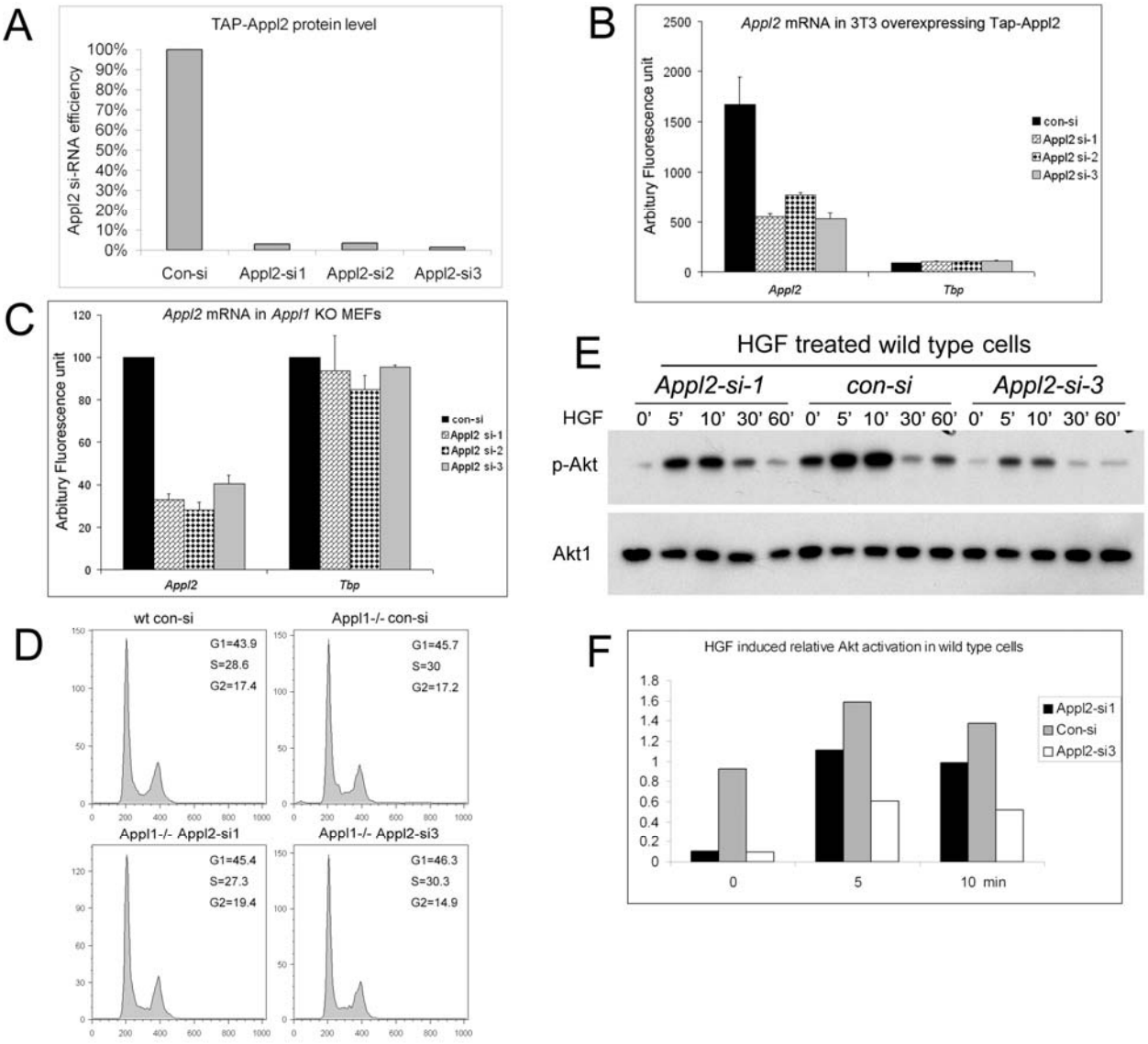

SUPPLMENTAL FIGURE8.

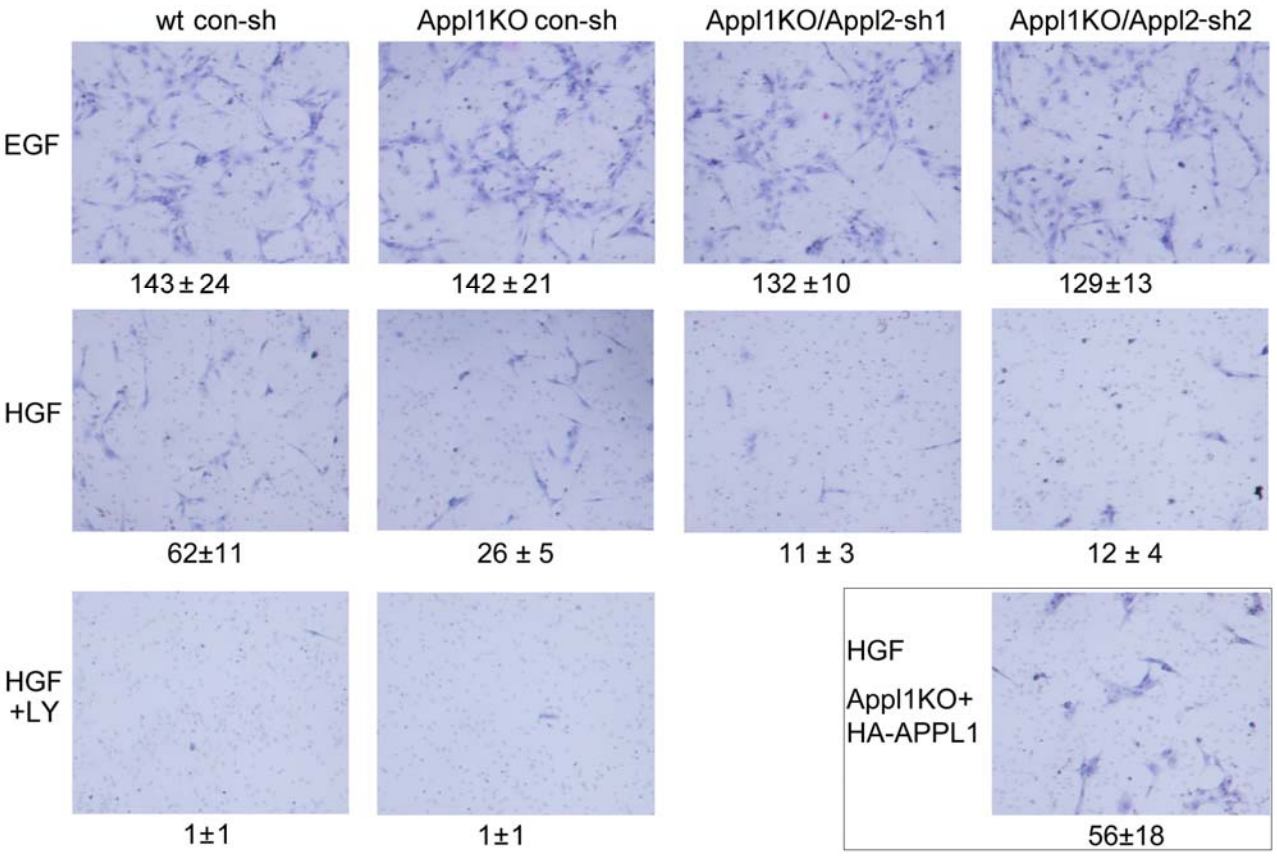

SUPPLMENTAL FIGURE 9.